12. A. N. Kiselev, "Magnetic measurements in shock waves," Fiz. Goreniya Vzryva, No. 6 (1975).
13. V. K. Golubev, S. A. Novikov, et al., "Mechanism of spallation of steels St. 3 and 12Kh18N10T in the temperature range 196-800°C," Probl. Prochn., No. 5 (1981).
14. V. N. German, V. I. Tsypkin, et al., "Behavior of steel Kh18N10T under the combined influence of shock loading and high-rate deformation," Probl. Prochn., No. 9 (1981).

EFFECT OF HEATING ON THE CLEAVAGE FRACTURE OF CERTAIN POLYMERIC COMPOSITES

V. K. Golubev, S. A. Novikov,
Yu. S. Sobolev, A. A. Khokhlov,
and N. A. Yukina

UDC 539.4

A successful combination of good specific mechanical properties and good thermophysical and dielectric characteristics is the reason for the broad use of polymeric composites as structural materials in high technology. However, the data available on the strength and failure of these materials under shock-wave loads is inadequate for optimizing the design of structures made of them. We can point only to the studies [1-5], which present isolated data on the conditions of cleavage failure of certain composites. There is almost no information for polymer materials on the effect of high temperature on cleavage failure, although high temperatures constitute one of the main factors affecting the service conditions of the structure. In this connection, we can cite only [6], which studied the effect of temperature on the cleavage fracture of several polymers. Here, we pose the problem of determining the conditions and character of cleavage failure of four typical polymeric composites: textolite, asbestos-textolite, glass-textolite, and glass-plastic AG-4.

The set-up of the tests was similar to [6]. The test specimens, in the form of disks 40 mm in diameter and 4 mm thick, were secured to an aluminum shield 8 mm thick. The specimens were shock-loaded by loading the shield with a 4-mm-thick aluminum plate accelerated to the required velocity by the detonation of a thin layer of explosive. The specimen was heated to 130°C through the shield by means of an electric heater. The specimen temperature was monitored with a Chromel–Alumel thermocouple. After the shock-wave tests, we visually inspected the specimens and prepared microsections of their longitudinal axial sections. The microsections were analyzed and photographed with optical equipment normally used in metallographic studies.

The methods used to obtain the materials, the conditions of their use, and their physicomechanical properties are described in [7]. Data on the density of the specimens, obtained by hydrostatic weighing, is shown in Table 1.

The test results are shown in Fig. 1 (a – textolite, b – glass-plastic, c – asbestos-plastic, d – glass-textolite). The velocity of the striker w and the temperature T correspond to the condition of the specimen after testing. The condition of the specimen was tentatively classified in accordance with three gradations: 1) absence of cleavage, correspondence of the specimen structure to the structure of the control specimen; 2) partial cleavage fracture – presence of cleavage damages visible on the microsection either unaided or at low magnification; 3) complete cleavage failure – presence of a main cleavage crack or direct separation of a cleaved layer of material. The characteristic time of mechanical loading of the specimens was 1.5 μsec, as in [6].

The estimates of the mechanical conditions of loading, characterized by the amplitude of the pressure in the compressive loading pulse, are based on the following assumptions. Table 2 gives parameters of the Hugoniot curves of certain composites in the form of linear D–u relations. The table also shows the ranges of mass velocity for which these relations were obtained. Comparison of the familiar Hugoniot curves of textolite and the binders permits us to suggest that the addition of up to 50% (by wt.) of a low-density filler such as

Moscow. Translated from Zhurnal Prikladnoi Mekhaniki i Tekhnicheskoi Fiziki, No. 6, pp. 140-145, November-December, 1987. Original article submitted September 9, 1986.

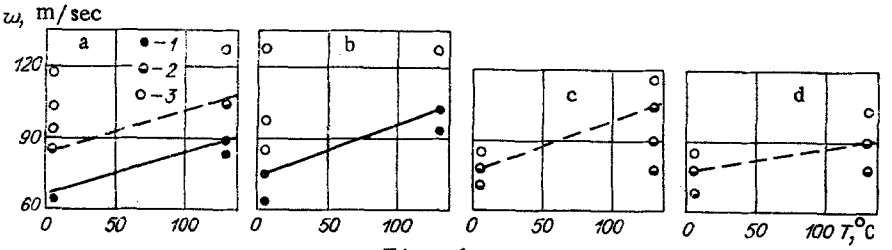

Fig. 1

TABLE 1

Material	ρ, g/cm³	p, GPa (T=0...20°C)	p, GPa (T=130°C)
Textolite	1,37	0,20—0,24	0,26—0,30
Asbestos-textolite	1,53	—0,24	—0,33
Glass-textolite	1,63	—0,25	—0,29
Glass-plastic	1,90	0,27—0,30	0,39—0,45

TABLE 2

Material	ρ, g/cm³	c_0, km/sec	λ	u, km/sec	Source
Textolite	1,36	2,65	1,49	0—2,1	[4]
Epoxy resin	1,19	2,64	1,66	0—2,4	[8]
» »	1,19	2,68	1,52	1,2—2,2	[1]
Phenolic resin	1,17	2,27	1,70	1,3—2,6	[1]
Quartz-phenol	1,66	3,02	1,01	0,7—2,4	[1]
Glass-textolite		3,0	1,88	0—0,6	[5]

cotton fabric to the resin does not lead to a significant change in the D−u relation of the resin. As regards composites in which the filler consists of glass fibers, in this case there is an increase in the parameter c_0 to 3.0 km/sec. This is the main parameter which characterizes shock-wave compressibility at low pressures. Also, as shown by examination of the results in [1], the values of c_0 for polymers and polymeric composites are generally located between their values of longitudinal c_l and volumetric c_b sonic velocity. We will evaluate these velocities for glass-plastic AG-4 having the maximum content of glass fibers. The evaluation involves the use of the elastic constants presented in [7] for unoriented material. Since the density of the specimens of glass-plastic we studied was as high as possible, we will take the maximum values for the Young's modulus E and shear modulus G. These values are equal to 14.5 and 5.2 GPa. We will also take the minimum value, 0.26, for the Poisson's ratio. For the sonic velocities we obtain $c_b = \sqrt{\frac{E}{3\rho(1-2\mu)}} = 2.31$ km/sec, $c_t = \sqrt{\frac{G}{\rho}} = 1.65$ km/sec, $c_l = \sqrt{c_b^2 + (4/3)c_t^2} = 2.99$ km/sec. Thus, c_0 for the investigated glass-plastic will be found in the range 2.3-3.0 km/sec. Thus, in light of the shortage of information on the shock-wave properties of specific materials and with the aim of uniformity, we will use c_0 = 2.6 km/sec for the composites studied here. This value serves as an adequate lower estimate for all of the materials. For the glass-filled composites, the actual value will be no greater than 15% above this value.

Considering that c_0 for aluminum is 5.3 km/sec, we can change over from the striker velocity w used in Fig. 1 to the pressure in the loading pulse $p = \rho_1 c_{01} w/(1 + \rho_1 c_{01}/\rho_2 c_{02})$, where the indices 1 and 2 pertain to the composite and the aluminum, respectively. The resulting approximate relation obtained between w and p for the investigated polymeric composites is shown in Fig. 2 (1 − textolite, 2 − asbestos-textolite, 3 − glass-textolite, 4 − glass-plastic). Using this relation and the original experimental results presented in Fig. 1, we can evaluate the critical mechanical loading conditions corresponding to cleavage failure of the composite. The load levels corresponding to the initiation of cleavage damages and to complete cleavage fracture and denoted by the solid and dashed lines in Fig. 1. Table 1 shows approximate ranges of the impulsive loading pressure corresponding to the critical conditions of cleavage failure for the test composites.

Some results of observation of the character of cleavage failure of the test specimens are shown in Figs. 3-6. We will point out the main features characteristic of each of the composites.

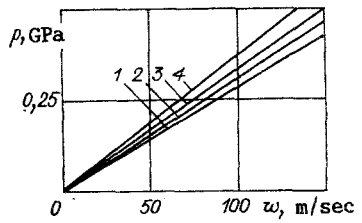

Fig. 2

Figure 3 shows longitudinal sections of textolite specimens tested at temperatures of about 0 (a, c) and 130°C (b, d). These specimens were loaded at impact velocities of 103 and 105 m/sec. Comparison of the macrostructural images (a, b, ×10) clearly shows the great dynamic strength of the material in the heated state. Whereas the macroscopic cleavage crack crosses nearly the entire specimen and travels along much of its lateral surface at about 0°C, the initial stage of macroscopic failure is seen only in part of the cross section at 130°C. The character of cleavage failure (c, d, ×70) is similar at both temperatures and is due to the nucleation and growth of cracks in layers of binder parallel to the plane. Meanwhile, fracture occurs in several parallel planes.

Figure 4 shows the appearance of a longitudinal section (a, ×10) and the character of cleavage (b, ×70) of asbestos-textolite specimens loaded at about 0°C at impact velocities of 85 and 77 m/sec, respectively. The cleavage microcracks are nucleated in the binder, while the main cleavage crack is formed between layers of asbestos cloth. Heating to 130°C leads to an increase in dynamic strength, but there is no change in the character of fracture.

Figure 5 shows the appearance of longitudinal sections of glass-textolite specimens loaded at about 0 (a, c) and 130°C (b, d) at impact velocities of 69 and 90 m/sec. The initial material contains fine pores which become fracture centers when the specimen is loaded. The binder frequently begins to crack at these pores in tests at about 0°C, while the pores increase in size at elevated temperatures and coalesce into a main crack. This can be seen in macro- (a, b, ×10) and microstructural (c, d, ×70) images of the longitudinal sections. Heating to 130°C in this case leads to an increase in dynamic strength and a change in the character of cleavage failure.

Figure 6 shows the appearance of the longitudinal section (a, ×10) and the character of cleavage failure (b, ×70) of specimens of glass-plastic AG-4 loaded at approximately 0°C at impact velocities of 85 and 128 m/sec. The cleavage cracks are nucleated and propagated in

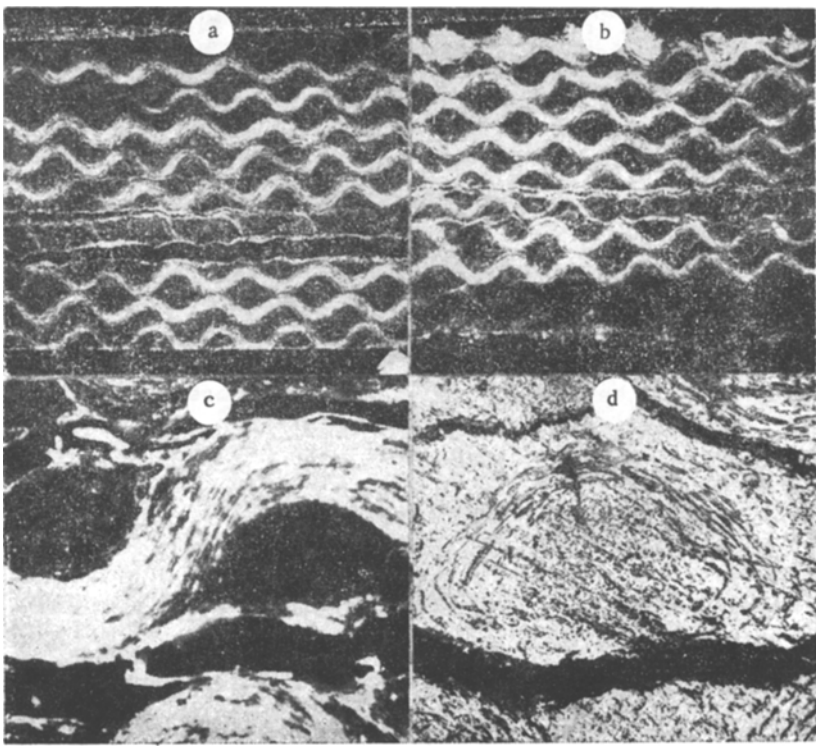

Fig. 3

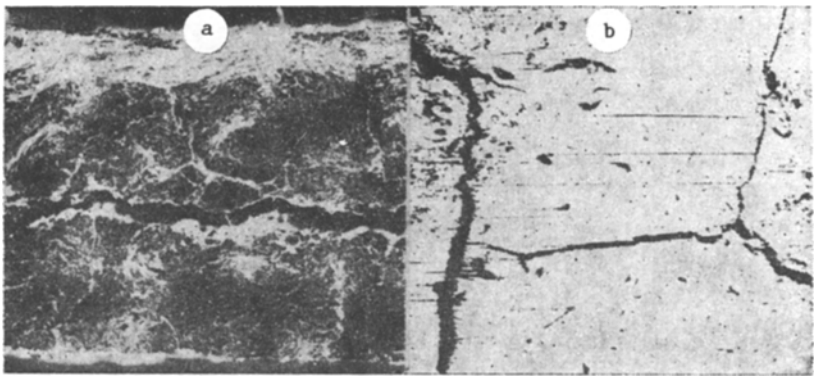

Fig. 4

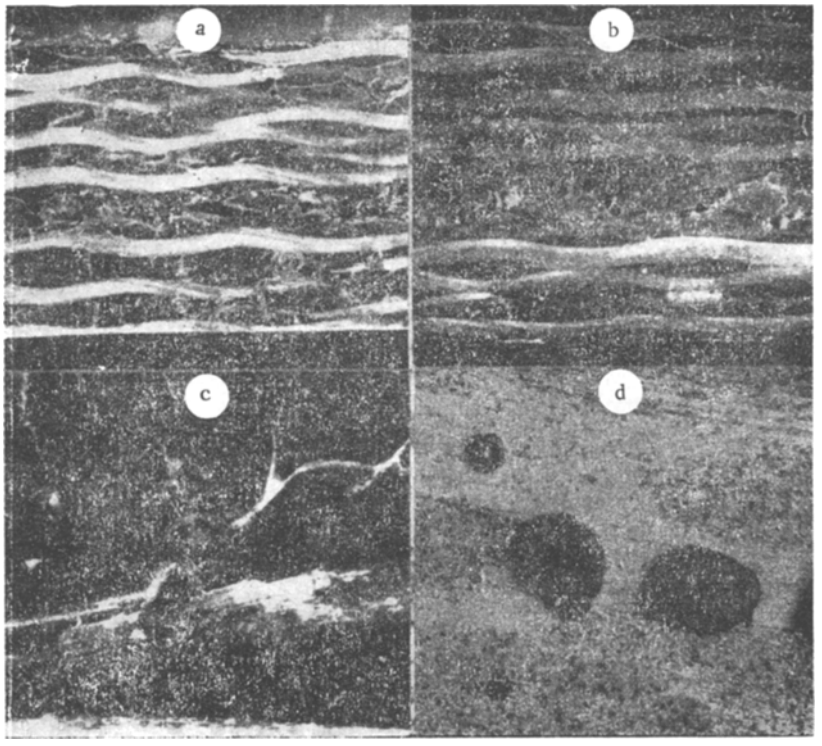

Fig. 5

the interlayers of binder. The character of failure of the glass-plastic does not change with heating to 130°C.

Thus, judging on the basis of the results obtained here, with a characteristic loading time of about 1.5 sec, the critical value of loading pressure corresponding to macroscopic cleavage failure of laminated plastic with a binder content of about 50% by wt. is approximately 0.24-0.25 GPa. Heating to 130°C leads to an increase in the critical pressure to about 0.29-0.33, depending on the type of material. An increase in the content of filler (glass fibers) and a reduction in the degree of orientation, as in the case of glass-plastic AG-4, leads to an increase in dynamic strength at both 0°C and elevated temperature. The similarity of the strength properties of textolites with different types of fillers is due to the fact that fracture occurs mainly in the binder, which consists of different phenol-formaldehyde and epoxy resins with similar physicomechanical properties. However, it must be noted that cleavage damages are nucleated in adhesive VK-3 – based on phenol-formaldehyde resin – when loaded by a pressure pulse of about 0.11 GPa, while heating to 130°C does not lead to any appreciable increase in strength. The same result was obtained in [6]. This indicates that the reinforcement plays the decisive role in regard to increases in the dynamic strength of polymeric composites, particularly at elevated temperatures.

Let us compare the results we obtained with well-known data on the cleavage failure of polymeric composites. Proceeding on the basis of two recorded changes [1] in the velocity

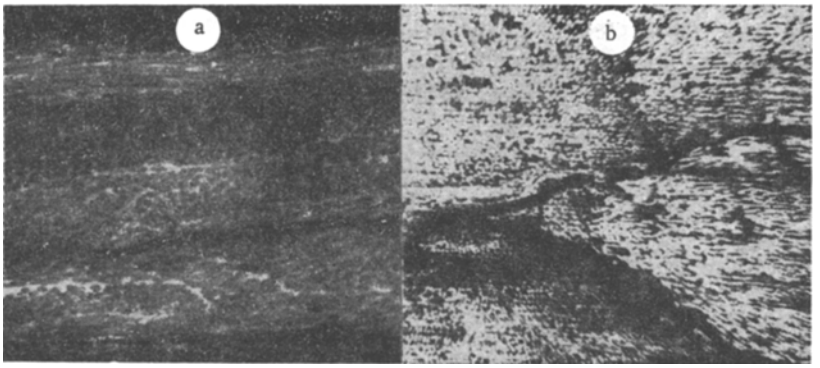

Fig. 6

of the free w_f of specimens of a quartz-phenol composite ("Refrasil"), we can estimate its cleavage strength $\sigma_s = \rho c_0 \Delta w_f/2$. Such an estimation gives a value of about 0.13 GPa. A similar estimate for glass-textolite [5], made on the basis of a recording of the pressure in a substrate as the cleaved layer decelerated on it, gave a value for cleavage strength in the range 0.14-0.22 GPa. On the other hand, the authors of [5] also determined the threshold value of impulsive loading pressure corresponding to the initial stage of cleavage failure. This value was 0.20-0.25 GPa. The estimates of negative pressure made in [4] for textolite, leading to its macroscopic cleavage failure when loaded by the explosion of a sheet charge of explosive, gave the values 0.2-0.3 GPa. Using a three-dimensional quartz-phenol composite as an example, the authors of [2] showed that the introduction of intermediate layers of glass fibers perpendicular to the plane of the specimen leads to an increase in resistance to cleavage by preventing the merging of cracks which form in the composite. The effect of loading time on the cleavage of polymeric composition was examined in [3], which presented results for a carbon-fiber plastic consisting of a three-dimensional structure of graphite fibers impregnated with phenolic resin. Here, we should note that whereas microscopic fracture began in the binder when loaded by a pressure pulse of about 0.2 GPa with a characteristic loading time of 1.5 μsec, a reduction in this time to 0.5 μsec was accompanied by a substantial increase in the critical loading pressure, to about 0.6 GPa.

In comparing the strength properties of polymeric composites under shock-wave and static loadings, we find that the fracture stress for grade B textolite in static tension of the weft, i.e., across the layers, is at least 45 MPa [7]. The cleavage strength in shock loading, however, is characterized by the range 0.20-0.24 GPa. Thus, the dynamic strength of textolite at approximately 0°C is more than four times greater than the static strength.

The fact that the dynamic strength of polymeric composites is considerably greater than their static strength (by a factor of 3-4) was noted in [9] in the tension of annular specimens at a rate of 150 sec^{-1}. This means that the phenomenon of dynamic strain-hardening is manifest at loading rates significantly below the rates associated with shock loading. It was found in [7] that the heating of laminated plastics to 120°C leads to a 25-27% reduction in the fracture stress in tension. Under shock loading, such heating has an effect of the same magnitude but the opposite direction — an increase in cleavage strength. Based on the above, we can conclude that it is very efficient to use polymeric composites in structures which are subject to the combined action of high temperatures and dynamic loads.

LITERATURE CITED

1. R. McEwen, S. Marsh, J. Taylor, et al., "Equation of state of solids from the results of shock-wave studies," in: High-Rate Impact Phenomena [Russian translation], Mir, Moscow (1973).
2. D. A. Shockey, L. Seaman, and D. R. Curran, "The influence of microstructural features on dynamic fracture," in: Metallurgical Effects at High Strain Rates, Plenum Press, New York, London (1973).
3. E. C. Goek and F. A. McClintock, "Fracture of graphite composites under shock loading," J. Appl. Phys., 46, No. 11 (1975).
4. V. K. Golubev, S. A. Novikov, and L. M. Sinitsyna, "Fracture of materials loaded by the explosion of a sheet charge of explosive," Zh. Prikl. Mekh. Tekh. Fiz., No. 2 (1981).
5. V. V. Astanin and V. I. Romanchenko, "Strength and compressibility of glass-plastic in impact," Mekh. Kompozitn. Mater., No. 4 (1984).

6. V. K. Golubev, S. A. Novikov, and Yu. S. Sobolev, "Effect of temperature on the cleavage fracture of polymers," Zh. Prikl. Mekh. Tekh. Fiz., No. 1 (1982).
7. V. M. Kataev et al. (eds.), Handbook of Plastics [in Russian], Vol. 2, Khimiya, Moscow (1975).
8. D. E. Munson and R. P. May, "Dynamically determined high-pressure compressibilities of three epoxy resin systems," J. Appl. Phys., 43, No. 3 (1972).
9. K. K. Chamis and G. T. Smit, "Effect of the environment and a high strain rate on composites used in engines," Aerokosmich. Tekhnika, 2, No. 9 (1984).

MULTIVALUED DISPLACEMENTS AND VOLTERRA DISLOCATIONS IN PLANE NONLINEAR ELASTICITY THEORY

L. M. Zubov and M. I. Karyakin

UDC 539.3

The problem is solved of determining the plane displacement field of a continuous medium by means of a unique finite strain tensor field given in a non-simply connected plane domain and satisfying the nonlinear compatibility equation. Given for the plane problem is a generalization of the classical Weingarten theorem to the case of large strains. An expression is obtained for the Burgers and Frank vectors of the Volterra dislocation (isolated defect) in terms of the finite strain tensor field. Given is a formulation of the plane problem of determining the stresses in a nonlinearly elastic body containing an isolated defect with given characteristics. An exact solution of the problems of a wedge disclination is found for a specific model of a nonlinearly elastic material. It is established that the stress field has no singularities on the disclination axis for a nonlinear formulation of the problem.

1. The plane strain of a continuous medium is described by the relationships

$$X_1 = X_1(x_1, x_2),\ X_2 = X_2(x_1, x_2),\ X_3 = x_3, \tag{1.1}$$

where x_k and X_k are Cartesian coordinates of points of the medium, respectively, before and after strain. We denote the coordinate directions by $\mathbf{e}_k$ (k = 1, 2, 3). We introduce complex coordinates and their associated vector bases [1-5]

$$\zeta = x_1 + ix_2,\ \bar{\zeta} = x_1 - ix_2,\ z = X_1 + iX_2,\ \bar{z} = X_1 - iX_2,$$
$$\mathbf{f}_1 = \bar{\mathbf{f}}_2 = \frac{1}{2}(\mathbf{e}_1 - i\mathbf{e}_2),\quad \mathbf{f}^1 = \bar{\mathbf{f}}^2 = \mathbf{e}_1 + i\mathbf{e}_2,\quad \mathbf{f}^3 = \mathbf{f}_3 = \mathbf{e}_3,\quad \mathbf{f}_k \cdot \mathbf{f}^n = \delta_k^n.$$

Here δ_k^n is the Kronecker delta. The plane strain (1.1) can evidently be given by using the complex-valued function

$$z = z(\zeta, \bar{\zeta}),\ X_3 = x_3. \tag{1.2}$$

The site gradient (distortion tensor) [2, 6] corresponding to the transformation (1.2) has the form

$$\mathbf{C} = \frac{\partial X_k}{\partial x_n}\mathbf{e}_n\mathbf{e}_k = \frac{\partial z}{\partial \zeta}\mathbf{f}^1\mathbf{f}_1 + \frac{\partial \bar{z}}{\partial \zeta}\mathbf{f}^1\mathbf{f}_2 + \frac{\partial z}{\partial \bar{\zeta}}\mathbf{f}^2\mathbf{f}_1 + \frac{\partial \bar{z}}{\partial \bar{\zeta}}\mathbf{f}^2\mathbf{f}_2 + \mathbf{f}^3\mathbf{f}_3. \tag{1.3}$$

A polar expansion of the site gradient results [7, pp. 59, 60] in the measure of the distortion $\mathbf{U}$ which is a symmetric positive-definite tensor of the second rank, and to an intrinsically orthogonal rotation tensor $\mathbf{A}$

$$\mathbf{C} = \mathbf{U}\cdot\mathbf{A},\ \mathbf{U} = \mathbf{G}^{1/2},\ \mathbf{G} = \mathbf{C}\cdot\mathbf{C}^T. \tag{1.4}$$

The Cauchy–Green finite strain tensor $\mathbf{E}$ is expressed in terms of the Cauchy strain measure $\mathbf{G}$ by the relationship [2, p. 24]

$$\mathbf{E} = (1/2)(\mathbf{G} - \mathbf{I}) \tag{1.5}$$

($\mathbf{I}$ is the unit tensor). For plane strain the rotation tensor has the representation

$$\mathbf{A} = (\mathbf{I} - \mathbf{e}_3\mathbf{e}_3)\cos\chi + (\mathbf{e}_1\mathbf{e}_2 - \mathbf{e}_2\mathbf{e}_1)\sin\chi + \mathbf{e}_3\mathbf{e}_3 = e^{i\chi}\mathbf{f}^1\mathbf{f}_1 + e^{-i\chi}\mathbf{f}^2\mathbf{f}_2 + \mathbf{f}^3\mathbf{f}_3, \tag{1.6}$$

Rostov-on-Don. Translated from Zhurnal Prikladnoi Mekhaniki i Tekhnicheskoi Fiziki, No. 6, pp. 146-152, November-December, 1987. Original article submitted July 30, 1986.

 0021-8944/87/2806-0934$12.50